Giant magnetoelectric coupling interaction in BaTiO3/BiFeO3/BaTiO3 trilayer multiferroic heterostructures

R. K. Kotnala, Rekha Gupta, and Sujeet Chaudhary

Citation: Applied Physics Letters **107**, 082908 (2015); doi: 10.1063/1.4929729
View online: http://dx.doi.org/10.1063/1.4929729
View Table of Contents: http://scitation.aip.org/content/aip/journal/apl/107/8?ver=pdfcov
Published by the AIP Publishing

Giant magnetoelectric coupling interaction in $BaTiO_3/BiFeO_3/BaTiO_3$ trilayer multiferroic heterostructures

R. K. Kotnala,[1,a)] Rekha Gupta,[1] and Sujeet Chaudhary[2]
[1]*CSIR-National Physical Laboratory, New Delhi 110012, India*
[2]*Department of Physics, Indian Institute of Technology Delhi, New Delhi 110016, India*

(Received 24 April 2015; accepted 16 August 2015; published online 28 August 2015)

Multiferroic trilayer thin films of $BaTiO_3/BiFeO_3/BaTiO_3$ were prepared by RF-magnetron sputtering technique at different thicknesses of $BiFeO_3$ layer. A pure phase polycrystalline growth of thin films was confirmed from X-ray diffraction results. The film showed maximum remnant electric polarization ($2P_r$) of 13.5 $\mu C/cm^2$ and saturation magnetization (M_s) of 61 emu/cc at room temperature. Thermally activated charge transport dominated via oxygen vacancies as calculated by their activation energy, which was consistent with current–voltage characteristics. Magnetic field induced large change in resistance and capacitance of grain, and grain boundary was modeled by combined impedance and modulus spectroscopy in the presence of varied magnetic fields. Presence of large intrinsic magnetoelectric coupling was established by a maximum 20% increase in grain capacitance (C_g) with applied magnetic field (2 kG) on trilayer having 20 nm $BiFeO_3$ layer. Substantially higher magnetoelectric coupling in thinner films has been observed due to bonding between Fe and Ti atoms at interface via oxygen atoms. Room temperature magnetoelectric coupling was confirmed by dynamic magnetoelectric coupling, and maximum longitudinal magnetoelectric coupling of 515 mV/cm-Oe was observed at 20 nm thickness of $BiFeO_3$. The observed magnetoelectric properties are potentially useful for novel room temperature magnetoelectric and spintronic device applications for obtaining higher voltage at lower applied magnetic field. © *2015 AIP Publishing LLC*. [http://dx.doi.org/10.1063/1.4929729]

Multiferroics is a significant class of materials that combine two or more ferroic order parameters, namely, the ferroelectricity, ferromagnetism, and ferroelasticity in a single phase.[1] The magnetoelectric (ME) coupling between magnetic and electrical order parameters in these multiferroics adds another functionality: possibility to control magnetic polarization by applying electric field (direct ME effect) and manipulation of electric polarization by magnetic field (converse ME effect).[2] Multilayer approach has been found to be most effective in influencing growth and physical properties of thin films. The maximum ME coupling interaction has been achieved in multiferroic heterostructures with alternate ferroelectric/ferromagnetic layers.[3,4] Multiferroic material Bismuth Ferrite (BFO) exhibits simultaneous existence of room temperature antiferromagnetism ($T_N = 643$ K) and ferroelectricity ($T_C = 1103$ K).[5] It has been very well explored that solid solutions of BFO with ferroelectric perovskite material $BaTiO_3$ (BTO) result in improved ferroelectric and magnetic properties.[6–9] However, there have been only few studies undertaken on epitaxial bilayer and multilayer thin films of BFO/BTO multiferroic composites.[10,11] In the layered composite thin film structures, magnetoelectric effects can be induced at the interface between two phases via strain between the two phases, change in oxygen stoichiometry, electronic correlations, interface bonding, exchange bias, and other physical phenomenon may also take place.[12] In our earlier work, we have reported interface induced improved magnetoelectric coupling in polycrystalline BFO/BTO bilayer films prepared by RF-sputtering.[13] In this letter, further improved magnetoelectric coupling of trilayer thin films of BTO/BFO/BTO has been reported by introducing two interfaces between BFO and BTO. Moreover, magnetoelectric coupling can be manipulated by changing the thickness of BFO layer. This study provides a direct evidence of high intrinsic magnetoelectric coupling interaction between BFO and BTO interface in the polycrystalline thin films which in not strain mediated.

Trilayer thin films of BTO/BFO/BTO were prepared on $Pt/TiO_2/SiO_2/Si$ (100) substrate by RF-magnetron sputtering technique. Targets of $BiFeO_3$ and $BaTiO_3$ were synthesized by conventional solid state reaction method. BTO layer was first deposited on $Pt/TiO_2/SiO_2/Si$ (100) substrate maintained at 650 °C followed by subsequent deposition of BFO layer on $BTO/Pt/TiO_2/SiO_2/Si$ (100) at the same substrate temperature. Top BTO layer was deposited on $BFO/BTO/Pt/TiO_2/SiO_2/Si$ (100) under similar conditions as the bottom layer. The deposition was carried out at 50 mTorr in a mixture of Ar and O_2 in the ratio of 4:1 with a base pressure of 3×10^{-6} Torr. The thickness of BTO film was kept fixed at 20 nm for both top and bottom layers, while BFO layer was deposited for different thicknesses of 20 nm (B-2), 40 nm (B-4), 60 nm (B-6), and 80 nm (B-8), respectively. Circular platinum top electrodes with diameter of 0.5 mm were sputtered on these trilayers to investigate electrical properties of thin films. Crystalline structure of thin films was analyzed by using X-ray Diffractometer (Phillips X-pert Pro) with CuK_α ($\lambda = 0.154$ nm) radiation. The dielectric measurements were carried out using LCR meter (Wayne Kerr 6500B), and

a)Author to whom correspondence should be addressed. Electronic addresses: rkkotnala@nplindia.org and rkkotnala@gmail.com. Telephone: 91-11-45608599. Fax: 91-11-45609310.

ferroelectric measurements were performed using a PE loop tracer. Magnetic measurements were carried out by VSM (Lakeshore 7304). Magnetoelectric measurements were performed on in-house ME setup.

Figure 1(a) illustrates XRD pattern of the trilayer BTO/BFO/BTO films recorded in θ–2θ mode. All the films were found to be in polycrystalline pure perovskite phase and no impurity phases were detected. The interface morphology of trilayer film was further analyzed by cross sectional FESEM image. See supplementary material for Fig. S1.[14] Sharp and defect free interface was observed between BFO and BTO phases. The quantitative elemental analysis of the interface was performed by EDX spectra.

Figure 1(b) represents the variation of leakage current density (J) as a function of electric field (E) for these trilayer films. Observed current density $\sim 10^{-4}$ A/cm^2 were found to be in close agreement to the reported values.[15–18] Leakage current in BFO thin films is attributed to the valance fluctuation of Fe ions between Fe^{2+} and Fe^{3+} states and migration of oxygen vacancies toward electrode resulting into the conduction under high electric fields.[19] High substrate temperature ($\sim$650 °C) and low oxygen partial pressure ($\sim 10^{-2}$ Torr) results in the formation of oxygen vacancies in trilayer films during sputtering. Conduction electrons can be released from neutralized oxygen vacancies via their ionization as written by following equation: $O_0 = \frac{1}{2} O_2 + \ddot{V} + 2e^-$, in Krogen-Vink notation. These conduction electrons can be further captured by Fe^{3+} ions resulting in their reduction to Fe^{2+} ions. Presence of Fe in both Fe^{2+} and Fe^{3+} oxidation states in BFO thin film deposited by same target material has been confirmed by XPS analysis in our earlier work.[13] It results in the hopping of electrons between two valence states of Fe and additionally such electrons are weakly bound to oxygen vacancies. It has been already reported that oxygen vacancies rather than Fe^{2+} contribute more to the leakage current.[20–23] Such process also results in creation of shallow level traps to electrons and this effect was further analyzed by studying the mechanism of current conduction involved in these films according to bulk limited and interface limited current conduction in ferroelectric thin films.[24–26] The conduction mechanisms in trilayer films were explored by logarithmic plots of the leakage current density versus applied electric field [log(J)/log(E)]. See supplementary material for Fig. S3.[14] For all the trilayer films, the plots were fitted well by linear segments with different slope values. At low electric field region, for all samples, the slope value (S) of $\sim$1.0 indicates ohmic conduction mechanism, which is dominated by thermally generated free electrons. However, the change in the slope value from $S \sim 1$ to $S \sim 2$ with an increase in applied electric field implies the change in conduction mechanism from ohmic to space charge limited conduction (SCLC). It may be noted that at lower electric fields, the injected carrier density is expected to be lower than thermally generated charge carriers resulting in ohmic behavior. With the increase in electric field, density of free electrons due to charge carrier injection becomes larger than the density of thermally generated electrons. Injected charge carriers get trapped at trap centers (oxygen vacancies) with the increase in applied electric field. Due to this, a field gradient is generated until all the traps are filled after which current rises abruptly as the field gradient is overcome with large change in slope as observed in these thin films. The observed reduction in leakage current with the increase in the thickness of BFO may be due to reduced oxygen vacancy concentration as thicker films have longer exposure to oxygen during sputtering resulting in the compensation of oxygen vacancies.

Magnetization hysteresis (M-H) loops measured at room temperature are shown in Fig. 1(c). All the films shows saturated ferromagnetic behavior with maximum saturation magnetization (M_s) of $\sim$61 emu/cc in B-2. The magnetization (M_s) value was found to be reduced with increasing thickness of BFO layer as 36 emu/cc in B-4, 23 emu/cc in B-6, and 19 emu/cc in B-8 sample. BFO is a G-type antiferromagnetic with spiral spin ordering of Fe^{3+} magnetic moments

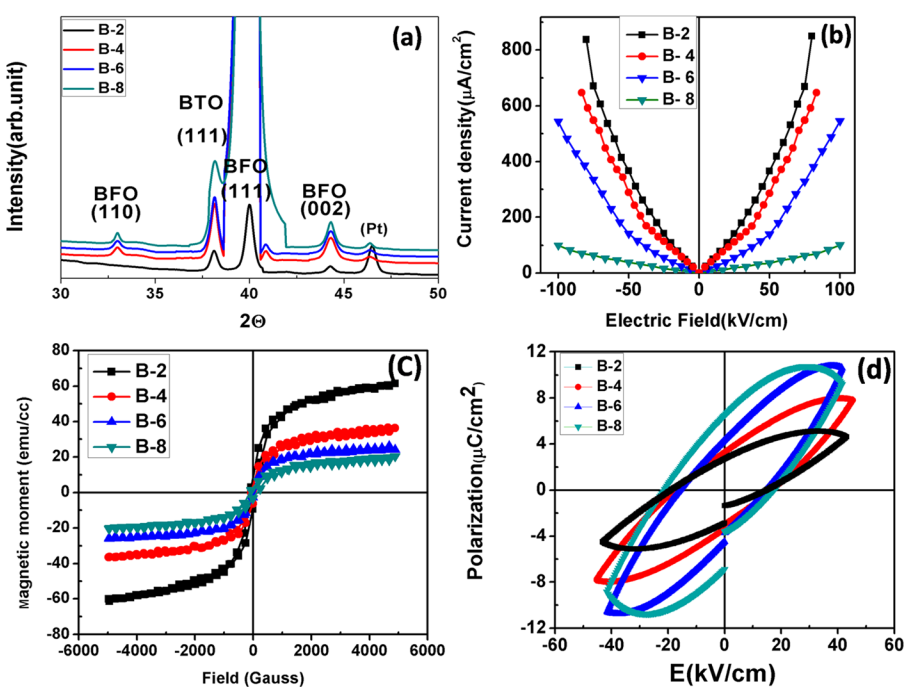

FIG. 1. (a) XRD patterns (θ-2θ scan) of BTO/BFO/BTO trilayer films having different BFO thicknesses on Pt/TiO_2/SiO_2/Si (100) substrate. (b) Current density vs electric field curves of BTO/BFO/BTO films having different BFO thicknesses. (c) Room temperature magnetization (M-H) loops of trilayer thin films at different BFO thicknesses. (d) Room temperature PE loops of BTO/BFO/BTO trilayer thin films having different BFO thicknesses.

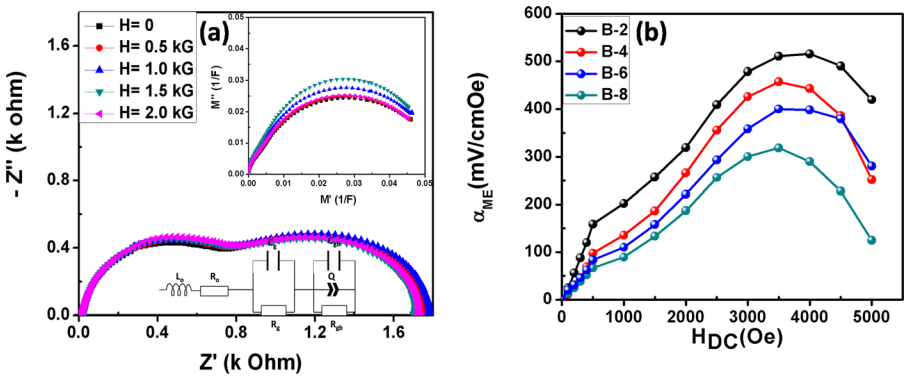

FIG. 2. (a) Magneto-impedance response of trilayer thin film (B-2) at room temperature and equivalent circuit used for fitting the impedance data. The inset represents the corresponding magneto-modulus plots recorded under different strengths of DC magnetic fields. (b) Magnetic field dependence of magnetoelectric coupling coefficient in longitudinal direction for BTO/BFO/BTO trilayer having different BFO layer thicknesses.

coupled ferromagnetically within (111) planes and antiferromagnetically between adjacent planes.[27] Disruption of spiral spin ordering at both interfaces of BFO sandwiched between BTO may result in induced weak ferromagnetism. The significantly enhanced saturation magnetization observed in these films implies the presence of ferromagnetic interaction between Fe^{2+} and Fe^{3+} ions. Exchange interaction between Fe^{2+} and Fe^{3+} ions mediated by oxygen vacancy (Fe^{2+}– Ö – Fe^{3+}) results in the ferromagnetic behavior.[28] Decreasing magnetization with increasing thickness of BFO layer can be accompanied by reduced oxygen vacancies, which mediate exchange interaction between Fe^{2+} and Fe^{3+} ions.

Figure 1(d) represents polarization hysteresis loops of trilayer films measured at 50 kV/cm applied electric field at 10 kHz frequency. The ferroelectric polarization was found to be improved with increasing thickness of BFO layer. Maximum remnant polarization ($2P_r$) was observed $\sim$13.5 $\mu C/cm^2$ in B-8, which systematically reduced to 9 $\mu C/cm^2$ in B-6, 7 $\mu C/cm^2$ in B-4, and 5.7 $\mu C/cm^2$ in B-2 film. Larger ferroelectric polarization in thicker films may be attributed to the reduced oxygen vacancy as also confirmed from current voltage characteristics.

Frequency dependent real (ε') and imaginary (ε'') parts of dielectric permittivity represented increased dielectric constant (ε') and decreased dielectric loss (ε'') with increasing thickness of BFO layer. See supplementary material for Fig. S4.[14] Larger value of dielectric loss in thinner samples represents higher conduction in these samples, which is in agreement with ferroelectric results. To further analyze migration kinetics of thermally activated charge carriers, activation energies were studied by fitting relaxation time corresponding to the loss peak by Arrhenius law as given by the equation $\tau_m = \tau_0 \exp\left(\frac{-E_a}{k_B T}\right)$, where τ_m is relaxation time corresponding to the loss peak, τ_0 is pre-exponential factor, E_a is activation energy for relaxation, k_B is Boltzmann's constant, and T is absolute temperature. Activation energies for conduction in temperature range of 298 K–428 K were calculated from ln τ vs 1/T plot. See supplementary material for Fig. S5.[14] In the trilayer film with 20 nm BFO layer, two distinct regions of activation energies were observed with $E_a \sim 0.24$ eV ($T < 353$ K) corresponding to second ionization energy of oxygen vacancy and $E_a \sim 0.39$ eV at higher temperature, which is close to the activation energy corresponding to the two site electron hopping between Fe^{2+} and Fe^{3+} ions.[29] The calculated activation energy $E_a \sim 0.26$ eV for B-2, $E_a \sim 0.19$ eV for B-4, and $E_a \sim 0.11$ eV for B-8 all over the investigated temperature range corresponds to the ionization energy of oxygen vacancies. It indicates the sizeable coupling between oxygen vacancy and Fe-ions through localized electrons in thinner films, which may be due to higher concentration of oxygen vacancies. This can result in localized polarization at defect sites and artificially enhanced magnetoelectric coupling values in the trilayer films. In order to recognize the presence of true magnetoelectric coupling in films, effect of magnetic field on the resistance and capacitance of the grains, grain boundary, and electrode–film interface was further studied. Complex impedance (-Z″ vs Z′) as well as complex modulus plots (M″ vs M′) were obtained under different applied magnetic fields as shown in Fig. 2(a). Imaginary part of impedance highlights the contribution from largest resistance element, while imaginary part of modulus picks out the contribution from smallest capacitance by suppressing all electrode polarization effects.[30] The measurements were carried out at small excitation voltage of 50 mV. The data were fitted with an equivalent circuit represented by two series RC-elements. The parasitic contributions from inductance and resistance of measurement wires and electrodes were accounted by series inductor (L_o) and resistor (R_o) in the circuit. Distributed impedance response observed from the depressed semicircles was accounted by constant phase element (Q) indicating departure from ideal Debye-type model. As highly capacitive grain boundaries were obtained from calculated parameters, so modulus plots are dominated by grain (bulk) capacitance representing single semicircle. See supplementary material for Tables S1-S4.[14] Two well resolved semicircles representing increase in both grain and grain boundary resistance (R_g and R_{gb}) with applied magnetic field were observed in B-2 film as shown in Fig. 2(a), while inset of Fig. 2(a) shows change in grain capacitance with applied magnetic field. A maximum 20% increase in grain capacitance (C_g) with applied magnetic field (2 kG) observed in B-2 sample confirms the presence of intrinsic ME coupling. The change in both grain capacitance (C_g) and grain boundary capacitance (C_{gb}) with applied magnetic field was observed to be suppressed with increasing thickness of BFO layer. See supplementary material for Fig. S6.[14] The calculated parameters are given in Table I. Intrinsic grain contribution to magnetocapacitance in thinner films can be due to hybridization between Ti 3d and exchange split Fe 3d orbital via oxygen 2p orbital at the interface resulting in changing polarization of grains with applied magnetic field.[30,31] The bonding between Fe and Ti

TABLE I. Electric, magnetic, and magnetoelectric coupling parameters of the trilayer thin films at different BFO thicknesses.

Composition	Remnant polarization $2P_r$ ($\mu C/cm^2$)	Magnetization M_s (emu/cc)	Magnetoelectric coupling coefficient α_{ME} (mV/cm Oe)	Magnetocapacitance (%)	
				Grain (C_g)	Grain boundary (C_{gb})
B-2	5.7	61	515	20	16.8
B-4	7.0	37	457	5.95	13.23
B-6	9.0	25	400	4.75	10.5
B-8	13.5	19	318	2.43	8.55

atoms at interface results in the magnetoelectric interaction between BFO and BTO at both interfaces. High magnetocapacitance in thinner films can be accounted for difference in oxygen surrounding of Fe atoms at the interface. It has been observed that oxygen deficient interface produces stronger magnetoelectric coupling due to strong bonding between Fe and O atoms, thus reducing hybridization between Fe and Ti atoms at the interface.[31] This results in higher magnetoelectric coupling as thinner films which have larger oxygen vacancies as observed by electrical and magnetic properties so they have intrinsically coupled Fe and Ti atoms resulting in the underlying magnetocapacitance. Presence of large grain boundary capacitance in thinner films is due to the accumulation of hopping electrons at grain boundaries of interface.[13] In the presence of applied electric field, the hopping electrons between Fe^{2+} and Fe^{3+} ions migrate through the grains and get accumulated at grain boundaries at interface. Interaction of these charges with applied magnetic field consequently results in the change in dynamic capacitance of grain boundary and results in the magnetocapacitance effect in films. Such kind of effect has been explained by Maxwell-Wagner (M-W) capacitor model consisting of two leaky capacitors connected in series.[32] The presence of magnetoelectric coupling was further confirmed by room temperature magnetoelectric coupling measurements.

Magnetoelectric coupling coefficient (α_{ME}) was measured in trilayer films by dynamic method. Thin films were biased with AC magnetic field (δH) of 10 Oe at 999 Hz and a DC magnetic field (H_o) was applied collinear to it. Longitudinal α_{ME} was determined by applying effective magnetic field ($H_o + \delta H$) perpendicular to the sample and measuring the output voltage by lock-in amplifier with a fixed phase relationship to the reference signal. Prior to the measurements, films were poled in 40 kV/cm electric field at 150 °C for 1 h. The α_{ME} was calculated using equation, $\alpha_{ME} = \frac{\delta V}{\delta H.t}$, where δV is the measured output voltage, δH is applied AC magnetic field, and t is the thickness of the sample. The maximum α_{ME} of ~515 mV/cm Oe was calculated for B-2 as shown in Fig. 2(b). With further increase in the thickness of BFO layer, α_{ME} reduced to ~457 mV/cm Oe for B-4, 400 mV/cm Oe for B-6, and to 318 mV/cm Oe for B-8 thin films. Significantly enhanced ME coupling in trilayer films prominently originates from bonding between Fe and Ti atoms at both interfaces via oxygen atom. Reduced oxygen vacancies with increasing thickness of BFO layer results in the decreasing value of ME coupling as oxygen rich interface weakens the bonding between Fe and Ti atoms.[31] The observed value of ME coupling coefficient in our samples is significantly larger than the reported value of 7 mV/cm Oe for single phase bulk $BiFeO_3$ sample and 124 mV/cm Oe for 0.9 BFO – 0.1 BTO ceramic composite thin films and bulk samples.[33–36] Such substantially high magnetoelectric coupling coefficient values obtained at room temperature paves the way to fabricate new type of electric-field controlled magnetic random access memory (MERAM), magnetoelectric sensors, voltage tunable RF/microwave signal processing devices, and spintronic devices

In conclusion, the trilayer multiferroic thin films of $BaTiO_3/BiFeO_3/BaTiO_3$ were prepared exhibiting simultaneous existence of saturation polarization and high saturation magnetization at room temperature. The influence of oxygen vacancy migration and hopping of electrons between Fe^{2+} and Fe^{3+} valence states on current conduction, magnetic as well as dielectric properties has been analyzed. Magnetic field induced large change in resistance and capacitance of grain and grain boundary was modeled by magneto-impedance spectroscopy. Room temperature existence of magnetoelectric coupling $(\alpha_{ME}) \sim 515$ mV/cm Oe in such films can be applicable in spintronic and memory device application for obtaining higher voltage at lower magnetic field.

The authors are grateful to the Director, "National Physical Laboratory" New Delhi for providing constant encouragement, motivation, and support to carry out this work.

[1]H. Schmid, Ferroelectrics **162**, 317 (1994).
[2]N. A. Spaldin and M. Fiebig, Science **309**, 391 (2005).
[3]H. Greve, E. Woltermann, R. Jahns, S. Marauska, B. Wagner, R. Knöchel, M. Wuttig, and E. Quandt, Appl. Phys. Lett. **97**, 152503 (2010).
[4]G. Sreenivasulu, L. Y. Fetisov, Y. K. Fetisov, and G. Srinivasan, Appl. Phys. Lett. **100**, 052901 (2012).
[5]G. Catalan and J. F. Scott, Adv. Mater. **21**, 2463 (2009).
[6]A. Singh, V. Pandey, R. K. Kotnala, and D. Pandey, Phys. Rev. Lett. **101**, 247602 (2008).
[7]K. Ueda, H. Tabata, and T. Kawai, Appl. Phys. Lett. **75**, 555 (1999).
[8]M. M. Kumar, A. Srinivas, and S. V. Suryanarayana, J. Appl. Phys. **87**, 855 (2000).
[9]R. Gupta, J. Shah, S. Singh, S. Chaudhary, and R. K. Kotnala, J. Nanopart. Res. **15**, 2004 (2013).
[10]P. Yang, K. M. Kim, Y. G. Joh, D. H. Kim, J. Y. Lee, J. S. Zhu, and H. Y. Lee, J. Appl. Phys. **105**, 061618 (2009).
[11]M. Lorenz, V. Lazenka, P. Schwinkendorf, F. Bern, M. Ziese, H. Modarresi, A. Volodin, M. J. Van Bael, K. Temst, A. Vantomme, and M. Grundmann, J. Phys. D: Appl. Phys. **47**, 135303 (2014).
[12]L. W. Martin, S. P. Crane, Y. H. Chu, M. B. Holcomb, M. Gajek, M. Huijben, C. H. Yang, N. Balke, and R. Ramesh, J. Phys.: Condens. Matter **20**, 434220 (2008).
[13]R. Gupta, S. Chaudhary, and R. K. Kotnala, ACS Appl. Mater. Interfaces **7**, 8472 (2015).
[14]See supplementary material at http://dx.doi.org/10.1063/1.4929729 for Figs. S1-S7 and Tables S1-S4.

[15]H. Yang, M. Jain, N. A. Suvorova, H. Zhou, H. M. Luo, D. M. Feldmann, P. C. Dowden, R. F. DePaula, S. R. Foltyn, and Q. X. Ji, Appl. Phys. Lett. **91**, 072911 (2007).
[16]G. W. Pabst, L. W. Martin, Y. H. Chu, and R. Ramesh, Appl. Phys. Lett. **90**, 072902 (2007).
[17]S. K. Singh, H. Ishiwara, and K. Maruyama, Appl. Phys. Lett. **88**, 262908 (2006).
[18]F. Yan, M. O. Lai, L. Lu, and T. J. Zhu, J. Phys. D: Appl. Phys. **44**, 435302 (2011).
[19]R. Ramesh and N. A. Spaldin, Nat. Mater. **6**, 21 (2007).
[20]X. Qi, J. Dho, R. Tomov, M. G. Blamire, and J. L. MacManus-Driscoll, Appl. Phys. Lett. **86**, 062903 (2005).
[21]X. H. Xiao, J. Zhu, Y. R. Li, W. B. Luo, B. F. Yu, L. X. Fan, F. Ren, C. Liu, and C. Z. Jiang, J. Phys. D: Appl. Phys. **40**, 5775 (2007).
[22]Y. W. Li, Z. G. Hu, F. Y. Yue, P. X. Yang, Y. N. Qian, W. J. Cheng, X. M. Ma, and J. H. Chu, J. Phys. D: Appl. Phys. **41**, 215403 (2008).
[23]H. Ihrig and D. Hennings, Phys. Rev. B **17**, 4593 (1978).
[24]M. Dawber, K. M. Rabe, and J. F. Scott, Rev. Mod. Phys. **77**, 1083 (2005).
[25]R. Waser and M. Klee, Integr. Ferroelectr. **2**, 23 (1992).
[26]X. G. Zhang and S. T. Pantelides, Phys. Rev. Lett. **108**, 266602 (2012).
[27]I. Sosnowska, T. P. Neumaier, and E. Steichele, J. Phys. C: Solid State Phys. **15**, 4835 (1982).
[28]D. Karmakar, S. K. Mandal, R. M. Kadam, P. L. Paulose, A. K. Rajarajan, T. K. Nath, A. K. Das, I. Dasgupta, and G. P. Das, Phys. Rev. B **75**, 144404 (2007).
[29]S. Hunpratub, P. Thongbai, T. Yamwong, R. Yimnirun, and S. Maensiri, Appl. Phys. Lett. **94**, 062904 (2009).
[30]J. T. S. Irvine, D. C. Sinclair, and A. R. West, Adv. Mater. **2**, 132 (1990).
[31]C. G. Duan, S. S. Jaswal, and E. Y. Tsymbal, Phys. Rev. Lett. **97**, 047201 (2006).
[32]M. K. Niranjan, J. P. Velev, C. G. Duan, S. S. Jaswal, and E. Y. Tsymbal, Phys. Rev. B **78**, 104405 (2008).
[33]G. Catalan, D. O. Neill, R. M. Bowman, and J. M. Gregg, Appl. Phys. Lett. **77**, 3078 (2000).
[34]J. M. Caicedo, J. A. Zapata, M. E. Gomez, and P. Prieto, J. Appl. Phys. **103**, 07E306 (2008).
[35]S. C. Yang, A. Kumar, V. Petkov, and S. Priya, J. Appl. Phys. **113**, 144101 (2013).
[36]R. Gupta, J. Shah, S. Chaudhary, and R. K. Kotnala, J. Alloys Compd. **638**, 115 (2015).